A LETTERS JOURNAL EXPLORING THE FRONTIERS OF PHYSICS

OFFPRINT

Dynamical manifestation of Hamiltonian monodromy

J. B. DELOS, G. DHONT, D. A. SADOVSKIÍ and B. I. ZHILINSKIÍ

EPL, **83** (2008) 24003

TAKE A LOOK AT THE NEW EPL

Europhysics Letters (EPL) has a new online home at
www.epljournal.org

Take a look for the latest journal news and information on:

- reading the latest articles, free!
- receiving free e-mail alerts
- submitting your work to EPL

www.epljournal.org

A Letters Journal Exploring the Frontiers of Physics

July 2008

EPL, **83** (2008) 24003
doi: 10.1209/0295-5075/83/24003

www.epljournal.org

Dynamical manifestation of Hamiltonian monodromy

J. B. Delos[1,2(a)], G. Dhont[2], D. A. Sadovskií[2] and B. I. Zhilinskií[2]

[1] *Physics Department, College of William and Mary - Williamsburg, VA 23185, USA*
[2] *Département de Physique, UMR 8101 du CNRS, Université du Littoral - 59140 Dunkerque, France, EU*

received 20 October 2007; accepted in final form 5 June 2008
published online 4 July 2008

PACS 45.50.-j – Dynamics and kinematics of a particle and a system of particles
PACS 45.05.+x – General theory of classical mechanics of discrete systems
PACS 03.65.Vf – Phases: geometric; dynamic, topological

Abstract – Hamiltonian monodromy —a topological property of the bundle of regular tori of a static Hamiltonian system which obstructs the existence of global action-angle variables— occurs in a number of integrable dynamical systems. Using as an example a simple integrable system of a particle in a circular box with quadratic potential barrier, we describe a time-dependent process which shows that monodromy in the static system leads to interesting dynamical effects.

Introduction. – One of the pleasures of research in physics is in examining a simple problem and finding something new and interesting in it. We also feel particularly motivated to look for a way of turning an abstract mathematical concept into a physical phenomenon that can potentially be observed experimentally. Both aspects are present in this letter.

We study here a very simple integrable Hamiltonian system that possesses the property called 'Hamiltonian monodromy'. This property is associated with the absence of global action-angle variables for the classical system, and with a local defect in the lattice of the joint spectrum of mutually commuting operators for the corresponding quantum system. We examine monodromy in a new perspective: we show that monodromy leads to nontrivial time-dependent evolution of the system. We also try to present the results so that physicists who are not familiar with Hamiltonian monodromy, a phenomenon known currently within a limited circle of specialists, can reproduce the calculation, and consider how our model setup can be transformed in order to observe the effect.

Monodromy was introduced in [1] as a topological property of the family of regular invariant tori of certain autonomous integrable Hamiltonian systems with two or more degrees of freedom. A number of simple classical mechanical systems, including the spherical pendulum, the Lagrange top, and others [2] are known to have this property. Quantum monodromy [3,4] was discovered in many fundamental quantum systems, such as the hydrogen atom in external fields [5–7], the H_2^+ molecular ion [8], systems with coupled angular momenta [9], rotating dipolar molecules in external electric field [10,11], rovibrational structure in molecules [12–17], collective vibrations of nuclei [18], or of Bose condensates [19] —to name a few.

Monodromy prevents classical and corresponding quantum systems from having global action-angle variables and global quantum numbers, respectively. In most cases, the presence of quantum monodromy was demonstrated by constructing the joint spectrum of mutually commuting observables, the energy and the angular momentum in the simplest case. In the (angular momentum, energy) domain, this spectrum forms a locally regular lattice of points with defects [3,4,9,20–23] which are the fingerprints of quantum and (via the correspondence principle) of classical Hamiltonian monodromy. Universality of such patterns in systems with monodromy reflects the topological origin of the phenomenon, and turns out to be useful in the analysis of complicated quantum spectra [14,16].

All of the above are "static" manifestations of monodromy in an unperturbed autonomous system. In this work we discuss a way to probe monodromy *dynamically*. We apply a small specific time-dependent perturbation to a static system with monodromy and we monitor the temporal evolution of the perturbed system. Since monodromy is a topological phenomenon, we look for interesting results that are (within certain limits) insensitive to the concrete form of the perturbation.

A simple system with monodromy. – All properties of the classical mechanical system studied here can be computed analytically in terms of elementary

(a) E-mail: jbdelo@wm.edu

functions. Its smooth analogue[1] is known as the "champagne bottle" [24] and it models such physical systems as doubly degenerate vibrations of a molecule near an unstable linear configuration [14–16]. Consider a classical particle of mass μ moving in two dimensions without friction inside a circular box of radius $\rho_{\max}$ with an axially-symmetric quadratic potential barrier

$$V_0 = \begin{cases} -a\,\boldsymbol{q}^2/2, & \text{when } |\boldsymbol{q}| \leqslant \rho_{\max}, \\ \infty, & \text{when } |\boldsymbol{q}| > \rho_{\max}, \end{cases} \tag{1}$$

where $\boldsymbol{q} = (x, y)$ are Cartesian coordinates of the particle, and $a > 0$. Denoting canonically conjugate momenta $\boldsymbol{p} = (p_x, p_y)$, the Hamiltonian of the system is

$$H_0(\boldsymbol{p}, \boldsymbol{q}) = \frac{1}{2\mu}\boldsymbol{p}^2 + V_0(\boldsymbol{q}). \tag{2}$$

This system is scalable and with no loss of generality we will assume $\mu = a = 1$; we will also use $\rho_{\max} = 3$ for all concrete computations. Denoting the four-vector $(x, y, p_x, p_y)^T$ as $\mathbf{u}$, the general solution to the linear equations of motion between the bounces, *i.e.*, so long as $\rho \equiv |\boldsymbol{q}| < \rho_{\max}$, is

$$\mathbf{u}(t) = S_{H_0}^{t-t_0}\, S_M^{\phi_0}\, \hat{\mathbf{u}}(m, E), \tag{3a}$$

where $S_{H_0}^t$ and S_M^ϕ are commuting matrices

$$S_{H_0}^t = \begin{pmatrix} \cosh t & 0 & \sinh t & 0 \\ 0 & \cosh t & 0 & \sinh t \\ \sinh t & 0 & \cosh t & 0 \\ 0 & \sinh t & 0 & \cosh t \end{pmatrix}, \tag{3b}$$

and

$$S_M^\phi = \begin{pmatrix} R^\phi & 0 \\ 0 & R^\phi \end{pmatrix} \quad \text{with} \quad R^\phi = \begin{pmatrix} \cos\phi & -\sin\phi \\ \sin\phi & \cos\phi \end{pmatrix}. \tag{3c}$$

Here t and ϕ denote time and polar angle $\tan^{-1}(y/x)$, respectively. Components of the initial vector $\hat{\mathbf{u}}$ are restricted by the conservation laws of energy $H_0(\boldsymbol{p}, \boldsymbol{q})$ and angular momentum $M(\boldsymbol{p}, \boldsymbol{q}) = xp_y - yp_x$ with respective values E and m. Since $\hat{\mathbf{u}}$ depends *only* on (E, m), two more constants (t_0, ϕ_0) are required to characterize the initial phase-space position of the particle at $t = 0$; the meaning of (t_0, ϕ_0) will become clear later. When the particle reaches $\rho = \rho_{\max}$, a hardwall reflection reverses the radial component p_ρ of $\boldsymbol{p}$, and the constants t_0 and ϕ_0 *change*. A typical trajectory is shown in fig. 1.

To uncover monodromy of this classical mechanical system, we can introduce local action-angle variables that

[1]Compared with a smooth confining potential (such as $V_0 = -a\,\boldsymbol{q}^2/2 + b\,\boldsymbol{q}^4/4$) the hard wall (1) has the effect of truncating the outer part of a smooth torus to a cylinder, but we can recover topological tori by identifying points on the two edges of the cylinder. With this identification, all trajectories are continuous. A representation of the initial and final torus is shown in fig. 5.

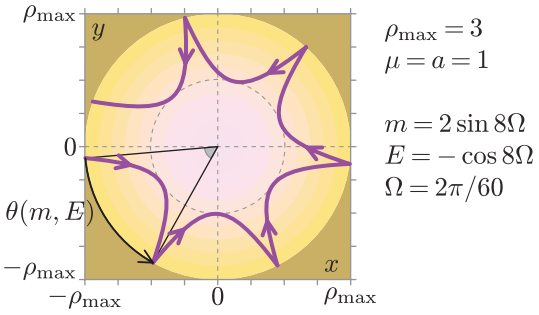

Fig. 1: Configuration space image of an unperturbed trajectory of a particle bouncing around a cylindrical barrier in eq. (1).

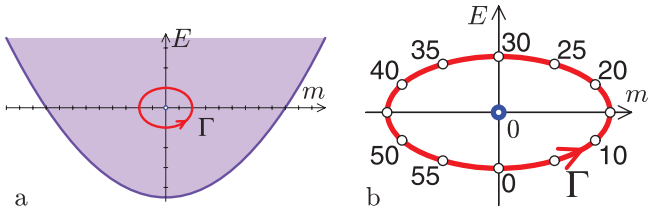

Fig. 2: Image of the energy-momentum map of the classical system with Hamiltonian H_0 (2). Light shade represents allowed set of regular (m, E) values, solid lower boundary corresponds to relative equilibria, the origin (0,0) of the energy-momentum plane is an isolated critical (m, E) value. Bold directed circle shows monodromy circuit Γ (4) surrounding the origin: (a) Γ within the set of regular (m, E) values, (b) snapshot time marks (cf fig. 3).

define coordinates on regular invariant tori Λ labelled by (angular momentum, energy) values (m, E). However, extending these coordinates globally to all regular tori $\Lambda_{m,E}$ is impossible: as we continue them along specific nontrivial closed paths Γ in the classically-allowed domain of regular (m, E) values (see fig. 2), we come back with a coordinate system which differs from the original one because one of our actions turns out to be a multivalued function of (m, E). We return to this phenomenon in more detail at the end of the letter.

Perturbed system. – The central idea of this work is that in order to observe a dynamical manifestation of monodromy, we should follow the motion of a *family* of trajectories, which we may call non-interacting particles. Furthermore, *additional forces are applied* which change the angular momentum m and energy E of each particle. Specifically, we want to perturb the system with Hamiltonian H_0 so that m and E of *every* particle evolve *continuously* around a closed counterclockwise directed path Γ encircling the origin of the (m, E) plane as shown in fig. 2. We call Γ a monodromy circuit.

In this paper we will not specify the perturbation as a force or as an additional term in the Hamiltonian, but instead we will characterize the perturbation by its desired results, *i.e.* by the desired flow in phase space. We assume that it is possible to perturb the system in such a way that *all* the particles in the family have the same value of

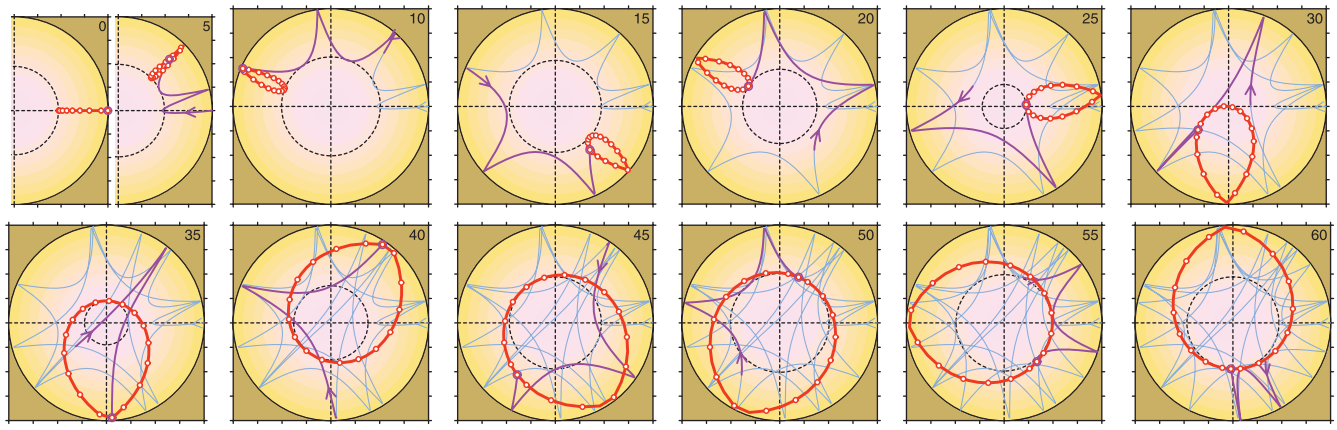

Fig. 3: A single trajectory and the instantaneous location of a family of particles in (x, y)-space shown in snapshots at time $t = t_k = 5, 10, \ldots, 60$, cf fig. 2 and eq. (4). The dashed circle indicates the currently forbidden region surrounding $x = y = 0$. The instantaneous location of one selected particle is marked by the large circle. The full trace of its trajectory for $0 \leqslant t \leqslant t_k$ is shown in each picture with the most recent section $t_{k-1} \leqslant t \leqslant t_k$ emphasized. Also shown are snapshots of the location of a family of particles, which all begin on the positive x-axis with $m = 0$ and $E = -1$, and which evolve around the same monodromy circuit. By $t = 5$, they form a loop in the (x, y)-plane, and as t increases, the loop steadily expands. After $t = 30$, the loop goes around the forbidden region. The evolution shows up most clearly in a movie, which was first presented at the 2006 APS DAMOP conference, and which is provided online (`pearl.gif` 1.5M).

angular momentum $m(t)$ and energy $E(t)$ at every instant t, and furthermore, perturbed trajectories are given by eq. (3) with (angular momentum, energy) values (m, E) in eq. (3a) varying with time.

One can think of a flock of automobiles racing in the circular stadium around the parabolic hill (1). All start with the same value of (m, E) but at different positions (t_0, ϕ_0) (see eq. (3)) and each automobile is required to use its engine and steering in such a way that the instantaneous values $m(t)$ and $E(t)$ evolve synchronously in the desired fashion prescribed by Γ.

Behaviour of the perturbed system. – Let a complete tour on Γ occur within the time interval $[t_\mathrm{t}, t_\mathrm{f}] = [0, 60]$. Taking $\Omega = 2\pi/60$ and a particular circuit

$$\Gamma : [0, 60] \to \mathbb{R}^2 : t \mapsto \begin{pmatrix} m(t) \\ E(t) \end{pmatrix} = \begin{pmatrix} 2 \sin \Omega t \\ -\cos \Omega t \end{pmatrix}, \qquad (4)$$

let particles begin with $m(0) = 0$ and $E(0) < 0$, and let $m(t)$ and $E(t)$ evolve along Γ until the final time $t_\mathrm{f} = 60$, when $m(60) = m(0) = 0$ and $E(60) = E(0)$.

One such particle (represented by the large hollow circle) is followed in fig. 3. Beginning with $y(0) = p_y(0) = 0$, $x(0) = \rho_\mathrm{max}$, $m(0) = 0$, $E(0) = -1$, which determine $p_x(0)$, the particle is moving initially on a radial line, climbing up the potential-energy barrier. As $m(t)$ increases, the particle begins moving around the enclosure counterclockwise. As $E(t)$ increases, the particle bounces in ever larger leaps, and then when $m(t)$ decreases, the pericentre of the path between bounces gets ever closer to the origin $(x = y = 0)$. At $t = 30$, $m(t)$ passes through zero while $E(t) > 0$, and at that instant the velocity of the particle points directly to (or from) the origin. Then with $m(t) < 0$ it begins bouncing clockwise. As $E(t)$ decreases, the angle subtended between bounces gets smaller, and finally at $t = 60$, $m(t) = 0$, $E(t) = E(0) = -1$, the particle is again bouncing on a radial line between the hard wall and the inner turning point.

Let us now launch a *family* of particles (hollow dots in fig. 3). Every particle begins with $y(0) = p_y(0) = 0$, $m(0) = 0$, and $E(0) = -1$, but they begin at different locations on the positive x-axis, between the inner turning point and ρ_max, while the magnitude of $p_x(0)$ is dictated by the energy $E(0)$. Thus at $t = 0$ all particles are moving either inward $(p_x(0) < 0)$ or outward $(p_x(0) > 0)$ on a straight radial line. When $m(t)$ increases, this family of particles forms in the (x, y)-plane a continuous closed loop with one point always touching the wall.

The essential result. – Now here is the important result. As m and E continue around Γ, the loop expands continuously. At the end $(t = 60)$, all particles return to negative energy and zero angular momentum, so they are all bouncing on straight radial lines between their inner turning point and the wall. However, *the loop of particles now encloses the classically forbidden region surrounding the origin* and no isoenergetic deformation could turn this loop into the initial loop! We observe, therefore, a topological transformation of the loop of initial conditions.

This result becomes quite remarkable once we realize that for *any* closed "placebo" circuit Γ' within the domain of regular (m, E) values, which starts with the same $m(0)$ and $E(0)$ but which does *not* encircle (0,0) (*i.e.*, Γ' is homotopic to a point), the topology of the loop will *not* change. Certainly, the loop may change its shape, it may end up at a different location, and individual particles may end up in different places on it, but the loop will remain homotopically equivalent to the initial loop.

The time-dependent phenomenon, in which an initial loop of particles evolves continuously in time into a

topologically different loop, is a dynamical manifestation of Hamiltonian monodromy. It is a robust phenomenon that does not depend on the specific realization of the monodromy circuit Γ in the (m, E) plane as long as Γ encircles the isolated critical value (0,0), and it is determined by the topological properties of the family of regular tori of the unperturbed (static) system governed by $H_0(\boldsymbol{p}, \boldsymbol{q})$. These properties are in turn defined by the type of the corresponding singular fibre $\Lambda_{0,0}$, *i.e.*, by the monodromy of the unperturbed system. In the rest of this letter, we describe in more detail how the evolution of particles is calculated, and we uncover why the resulting transformation is related to Hamiltonian monodromy.

Computation of perturbed trajectories. – We give more details on computing fig. 3. We assume that under our hypothetical perturbation, trajectories of particles are given by the formulae (3) for the unperturbed motion in which parameters m and E now vary with time. Returning to eq. (3), note that all dependence of the trajectory on (m, E) is contained in the vectors $\hat{\mathbf{u}}(m, E)$. Let $\Lambda_{m,E}$ be the torus (see footnote [1]) defined by $M(\boldsymbol{p}, \boldsymbol{q}) = m$ and $H_0(\boldsymbol{p}, \boldsymbol{q}) = E$. The vector $\hat{\mathbf{u}}(m, E)$ selects a point which serves as the origin of coordinates on this torus. For the circuit in eq. (4), we have chosen a smooth $\hat{\mathbf{u}} = \hat{\mathbf{u}}(t) = (\hat{x}(t), 0, 0, \hat{p}(t))$ with

$$\hat{x}(0) = -\hat{x}(60) = \rho_{\min}(m(0),\ E(0)), \tag{5a}$$

$$\hat{x}(t) = \operatorname{sgn}(m(t))\rho_{\min}(m(t),\ E(t)), \quad \text{for } 0 < t < 60, \tag{5b}$$

$$\hat{p}(t) = p_{\min}(m(t),\ E(t)) \geqslant 0, \quad \text{for } 0 \leqslant t \leqslant 60, \tag{5c}$$

where $\rho_{\min}(m, E)$ and $p_{\min}(m, E)$ are obtained by solving

$$|m| = \rho_{\min}\, p_{\min} \quad \text{and} \quad E = \tfrac{1}{2}\,(p_{\min}^2 - \rho_{\min}^2). \tag{5d}$$

The point $\hat{\mathbf{u}}$ is the *pericentre* of a *reference orbit*, which is the unperturbed trajectory on $\Lambda_{m,E}$ starting on the wall $|\boldsymbol{q}| = \rho_{\max}$ at time $-\tau/2$ and polar angle $-\theta/2$ and coming back to the wall at time $\tau/2$ and angle $\theta/2$ (fig. 4). The time $\tau = \tau(m, E)$ between bounces or the *period of first return*, and the angle $\theta = \theta(m, E)$ subtended between bounces, or the *rotation angle*, are given (for $\mu = a = 1$) by, respectively,

$$\tau(m, E) = \cosh^{-1} \frac{\rho_{\max}^2 + E}{c} \tag{6a}$$

and

$$\theta(m, E) = \tan^{-1}\left(\frac{E + c}{m}\sqrt{\frac{\rho_{\max}^2 + E - c}{\rho_{\max}^2 + E + c}}\right), \tag{6b}$$

where $c(m, E) := |E + \mathrm{i}\, m| = \sqrt{E^2 + m^2} \geqslant 0$. For $c(m, E) \ll \rho_{\max}^2$ we have simple asymptotic expressions

$$\tau(m, E) \approx \log 2\rho_{\max}^2 - \log|E + \mathrm{i}\, m| + \ldots, \tag{7a}$$

$$\theta(m, E) \approx \pi - \arg(E + \mathrm{i}\, m) + \ldots. \tag{7b}$$

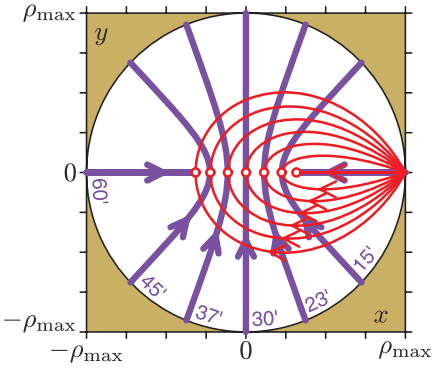

Fig. 4: Thick lines: (x, y)-images of reference orbits at various (m, E) corresponding to times on the monodromy circuit Γ (fig. 2). Thin lines: when the reference orbits are modified by the flow under M (rotation by $-\theta(m, E)$) they become closed fundamental loops γ_2 on the torus, shown in projection here.

All other unperturbed trajectories on $\Lambda_{m,E}$ differ in the initial position of the particle which is specified in eq. (3) by $t_0 \in [-\frac{1}{2}\tau, +\frac{1}{2}\tau)$ and $\phi_0 = [0, 2\pi)$. This describes the trajectory between bounces.

When the particle bounces off the wall, we simply augment t_0 and ϕ_0 by τ and θ, respectively, and continue the next smooth segment of the trajectory, as in fig. 1. On each such segment, the particle arrives at the pericentre at time t_0 and angle ϕ_0. So it follows that for a segment which begins after a bounce at time t_b and longitude ϕ_b,

$$t_0 = t_\mathrm{b} + \tfrac{1}{2}\tau(m, E) \quad \text{and} \quad \phi_0 = \phi_\mathrm{b} + \tfrac{1}{2}\theta(m, E). \tag{8}$$

As the system goes around the monodromy circuit, m and E change with time, so between bounces, we continue the trajectory using eq. (3) with fixed t_0 and ϕ_0, and with $\hat{\mathbf{u}}(m, E)$ varying according to eq. (4) and (5a). When the particle hits the wall at time t_b and longitude ϕ_b, which we can determine numerically, we find the new t_0 and ϕ_0 for the next segment by combining (8) and (4) and using instantaneous values $\tau(m(t_\mathrm{b}), E(t_\mathrm{b}))$ and $\theta(m(t_\mathrm{b}), E(t_\mathrm{b}))$. For this to work, we must use smooth and therefore necessarily multivalued functions $\hat{p}$, $\hat{x}$ and θ correctly along Γ, *e.g.*, we have $\hat{x}(60) = -\hat{x}(0)$ and $\theta(60) = \theta(0) + 2\pi$. This completes the description of our dynamical realization of the monodromy circuit in figs. 2, 3.

Relation to Hamiltonian monodromy. – Why does this topological change occur? A naive explanation can be supplied by noticing that at the time $t = 30$, when $m = 0$ and $E > 0$, one point on the continuous loop (not necessarily a particle in the discrete family) in fig. 3 touches the origin $x = y = 0$, *i.e.*, at that instant there exists one trajectory in this continuous family that passes through. By a continuity argument, the whole loop "slips" through the origin and over the barrier.

Understanding the origins of this phenomenon, we get into some recent advances in classical mechanics. The change which we observe is related to the monodromy

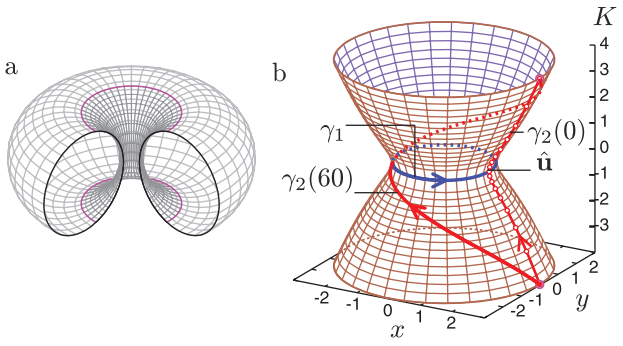

Fig. 5: (a) Immersion in $\mathbb{R}^3$ of a regular torus $\Lambda_{m,E}$ of the system with Hamiltonian H_0 (dark) and its smooth analogue (gray); the upper and lower circular edges (bold) are to be identified. (b) Initial and final loops $\gamma_2(0)$ and $\gamma_2(60)$ on the torus $\Lambda_{0,-1}$ immersed in $\mathbb{R}^3$ with coordinates x, y, and $K = \frac{1}{2}\boldsymbol{q}\cdot\boldsymbol{p}$.

of the underlying unperturbed integrable Hamiltonian system with first integrals H_0 and M. Monodromy characterizes how the regular tori of this system fit together. Specifically, we consider the set of regular tori $\Lambda_{m,E}$ with (m, E) on circuit Γ (eq. (4)), *i.e.*, the torus bundle over Γ. Local action-angle variables define coordinates on $\Lambda_{m,E}$ and tori in its neighbourhood, a local isomorphism which we can use to establish a *connection* between the coordinates on $\Lambda_{(t)} = \Lambda_{m(t),E(t)}$ as we go from the initial torus $\Lambda_{(0)}$ to the final torus $\Lambda_{(60)}$. These tori $\Lambda_{(0)}$ and $\Lambda_{(60)}$ are the same, but the initial and final *coordinate systems* on them differ. The difference is given by a monodromy matrix, which is a matrix in $\mathrm{SL}(2,\mathbb{Z})$. Having fixed the origin $\hat{\mathbf{u}}$ of the coordinates on $\Lambda_{m(t),E(t)}$, we can now pass coordinate axes through this origin using particular representatives γ_1 and γ_2 of cycles $[\gamma_1]$ and $[\gamma_2]$ of the fundamental group π_1 of $\Lambda_{m(t),E(t)}$. One such fundamental loop γ_1 is readily available on all tori. It is the orbit of the flow obtained from Hamiltonian $M(\boldsymbol{p}, \boldsymbol{q})$ and is given by

$$\gamma_1 : \mathbb{S}^1 \to \Lambda_{m,E} : \phi \mapsto S_M^{\phi}\hat{\mathbf{u}}(m, E). \tag{9a}$$

This loop γ_1 projects to configuration space as a counterclockwise path around the origin.

The second fundamental loop γ_2 has to be constructed continuously as we advance on Γ, *i.e.*, as t in eq. (4) goes from 0 to 60 (fig. 4 and 5). On the torus $\Lambda_{(0)}$, we can take $\gamma_2(0)$ to be the reference orbit itself, which goes from $x = \rho_{\max}$, $p_x = -p_{\max}$ to the inner turning point and back out to $x = \rho_{\max}$, $p_x = p_{\max}$ always with $y = p_y = 0$. However, on all other tori the reference orbits are not closed (fig. 4). On these we construct γ_2 by combining the reference orbit on $\Lambda_{(m,E)}$ with a cylindrical flow that compensates the change in angle $\theta(m, E)$ subtended by the orbit:

$$\gamma_2 : [-\tfrac{1}{2}, \tfrac{1}{2}] \to \Lambda_{m,E} : \xi \mapsto S_M^{-\xi\theta}\, S_{H_0}^{\xi\tau}\, \hat{\mathbf{u}}. \tag{9b}$$

Now $\xi = -\frac{1}{2}$ and $\xi = \frac{1}{2}$ represent the same point at the wall, so eq. (9b) describes a closed loop at each (m, E). As (m, E) change along Γ, that loop changes continuously. Since the reference orbit changes when we go around Γ (because $\hat{x}$ changes sign) and also θ changes from 0 to 2π, the final loop γ_2 must be different from the initial one. The resulting continuous family $\gamma_2(t)$ is shown in fig. 4, and we can see there and in fig. 5 right that the initial $\gamma_2(0)$ and final $\gamma_2(60)$ are not homotopic. In fact, since γ_1 is directed counterclockwise, $\gamma_2(60) = \gamma_2(0) - \gamma_1(0)$.

For the unperturbed (static) system, this has several consequences. Most importantly, this system cannot have action variables defined globally. Indeed the values $\mathcal{J}_1$ and $\mathcal{J}_2$ of actions are computed as integrals along respective cycles γ_1 and γ_2. So we have one globally defined action with $\mathcal{J}_1(m, E) = 2\pi\, m$, while $\mathcal{J}_2(m, E)$ is *multivalued*. In fact from the differential $\mathrm{d}\mathcal{J}_2 = \tau(m, E)\,\mathrm{d}E - \theta(m, E)\,\mathrm{d}m$, which is closed but not exact, we can obtain that for $c(m, E) \ll \rho_{\max}^2$

$$\mathcal{J}_2(m, E) \approx E + E\,\tau(m, E) - m\,\theta(m, E) + \ldots \tag{10}$$

For the dynamical system driven in time around the monodromy circuit, the particles starting on torus $\Lambda_{(0)}$ form a loop $\tilde{\gamma}_2(0)$ that is identical to $\gamma_2(0)$, and they end up forming a loop $\tilde{\gamma}_2(60)$ that is homotopic to $\gamma_2(60)$. This happens because the perturbation establishes a continuous *dynamical* connection that is similar to the static connection used in constructing $\gamma_2(t)$ (eq. (9b)) for the static system. Hence the similarity between the loops in figs. 3 and 4. Moreover, our calculations indicate that in the "slow" limit[2] of $\Omega \ll 1/\tau$ the loops $\tilde{\gamma}_2(t)$ and $\gamma_2(t)$ become identical.

Discussion. – Monodromy of our system is caused by the presence of the isolated critical fibre $\Lambda_{0,0}$ which includes the focus-focus equilibrium $\boldsymbol{q} = \boldsymbol{p} = 0$. The dynamics of a single particle on tori near such a fibre can be quite remarkable [27,28], but that single-particle behaviour cannot be related directly to monodromy. From this point of view, our essential contribution is that we must follow a collective time-dependent evolution of several particles.

We also like to relate our work to the setup in the geometric phase theories, see [26] and references therein. There is no direct connection between Hamiltonian monodromy and geometric phase, but they share certain common aspects [9,29]: in both cases, i) we study the structure of a regular toric fibration Φ with base space B by taking a closed loop $\Gamma \subset B$ and connecting the fibres over Γ; ii) following this connection, we look at what happens after we complete a tour on Γ. However, we deal here with Φ defined by the flow of a single Hamiltonian system and our B is the two-dimensional space of the regular values (m, E) of first integrals (shaded area in fig. 2 without the boundary and point 0). B is not simply

[2] When the motion around the monodromy circuit is much slower than the radial motion of the particles it can be called "adiabatic". However, contrary to, for example, [25,26], the values E and m, and those of local actions evolve with time even in this limit.

connected, we use a non-contractible Γ, and monodromy is non-trivial. In the geometric phase theories, B is a space of external parameters and Φ is of a more general kind. In the simplest situation, the topology of B may be that of an open ball and Γ may be homotopic to a point, and furthermore, both Φ and the torus bundle over Γ may have trivial topology, that of $B \times \mathbb{T}^2$ and $\mathbb{S}^1 \times \mathbb{T}^2$, respectively. In other words, monodromy is a topological phenomenon, while geometric phase is primarily a geometric phenomenon related to the curvature of B.

Specifically, the Berry-Hannay *angle* [26] gives the resulting change of the *angle* variable after a tour on Γ. It can occur already in one degree of freedom (for an $\mathbb{S}^1$ bundle over Γ). In two degrees of freedom, the initial and final coordinate systems on the 2-torus Λ may differ not only by the origin shift, which in our case is given by $\hat{\mathbf{u}}(60) - \hat{\mathbf{u}}(0)$ in (3) and (5), but also by an $\mathrm{SL}(2,\mathbb{Z})$ transformation of the basis. If the latter is the identity, we have trivial monodromy but we may still accumulate a geometric phase. Monodromy deals solely with the affine $\mathbb{Z}^2$ structure on Λ and homology $H_1(\Lambda)$; geometric phase is related to fixed origin coordinates. To measure the Hannay angle, we may compare positions of our particles on the initial and final loops. To uncover monodromy, we consider what happened to the loop as a whole and whether it became a qualitatively different loop. So the effect that we are after in this work is both 'cruder' and more robust.

Conclusion. – We have explained how to probe the monodromy of an autonomous (static) classical integrable system using a time-dependent dynamical process. Applying a time-dependent perturbation which forces the system to evolve in the energy-momentum plane along a closed circuit Γ, and following the collective evolution of a family of perturbed trajectories situated initially along a fundamental loop of a regular torus of the static system, we observed the modification of this loop of initial conditions into a topologically (homotopically) different final loop on the same torus. The transformation does not depend on the details of the dynamical processes used. It is determined entirely by the requirement for Γ to encircle the isolated critical energy-momentum value (0,0) and by the type of the singular fibre of the static system which corresponds to (0,0). From this study, we can infer a general result: a nontrivial connection between fundamental loops defined on a family of tori of an autonomous system leads to a nontrivial topological behaviour of a family of trajectories evolving in time through that family of tori.

* * *

This work was supported in 2005–2007 by the Région Nord–Pas-de-Calais and the NSF. We thank Prof. R. G. Littlejohn for his comment on the manuscript.

REFERENCES

[1] Duistermaat J. J., *Commun. Pure Appl. Math.*, **33** (1980) 687.
[2] Bates L. M. and Cushman R. H., *Global Aspects of Classical Integrable Systems* (Birkhäuser, Basel) 1997.
[3] Cushman R. H. and Duistermaat J. J., *Bull. Am. Math. Soc.*, **19** (1988) 475.
[4] Vũ Ngọc S., *Commun. Math. Phys.*, **203** (1999) 465.
[5] Cushman R. H. and Sadovskiĭ D. A., *Europhys. Lett.*, **47** (1999) 1; *Physica D*, **142** (2000) 166.
[6] Schleif C. R. and Delos J. B., *Phys. Rev. A*, **76** (2007) 013404.
[7] Efstathiou K., Sadovskiĭ D. A. and Zhilinskiĭ B. I., *Proc. R. Soc. London, Ser. A*, **463** (2007) 1771.
[8] Waalkens H., Dullin H. R. and Richter P. H., *Physica D*, **196** (2004) 265.
[9] Sadovskiĭ D. A. and Zhilinskiĭ B. I, *Phys. Lett. A*, **256** (1999) 235; Grondin L., Sadovskiĭ D. A. and Zhilinskiĭ B. I., *Phys. Rev. A*, **65** (2001) 012105.
[10] Kozin I. N. and Roberts R. M., *J. Chem. Phys.*, **118** (2003) 10523.
[11] Arango C. A., Kennerly W. W. and Ezra G. S., *Chem. Phys. Lett.*, **392** (2004) 486; *J. Chem. Phys.*, **122** (2005) 184303.
[12] Cushman R. H., Dullin H. R., Giacobbe A., Holm D. D., Joyeux M., Lynch P., Sadovskiĭ D. A. and Zhilinskiĭ B. I., *Phys. Rev. Lett.*, **93** (2004) 024302.
[13] Giacobbe A., Cushman R. H., Sadovskiĭ D. A. and Zhilinskiĭ B. I., *J. Math. Phys.*, **45** (2004) 5076.
[14] Winnewisser M., Winnewisser B. P., Medvedev I. R., De Lucia F. C., Ross S. C. and Bates L. M., *J. Mol. Struct.*, **798** (2006) 1.
[15] Child M. S., Weston T. and Tennyson J., *Mol. Phys.*, **96** (1999) 371.
[16] Zobov N. F., Shirin S. V., Polyansky O. L., Tennyson J., Coheur P.-F., Bernath P. F., Carleer M. and Colin R., *Chem. Phys. Lett.*, **414** (2005) 193.
[17] Joyeux M., Sadovskiĭ D. A. and Tennyson J., *Chem. Phys. Lett.*, **382** (2003) 439.
[18] Macek M., Cejnar P., Jolie J. and Heinze S., *Phys. Rev. C*, **73** (2006) 014307.
[19] Waalkens H., *Europhys. Lett.*, **58** (2002) 162.
[20] Zhilinskiĭ B. I., *Acta Appl. Math.*, **87** (2005) 281.
[21] Zhilinskiĭ B. I., in *Topology in Condensed Matter*, Vol. **150** (Springer-Verlag, Berlin) 2006, p. 165.
[22] Nekhoroshev N. N., Sadovskiĭ D. A. and Zhilinskiĭ B. I., *Ann. Henri Poincaré*, **7** (2006) 1099.
[23] Bolsinov A. V., Dullin H. R. and Veselov A. P., *Commun. Math. Phys.*, **264** (2006) 583.
[24] Bates L. M., *J. Appl. Math. Phys.*, **42** (1991) 837.
[25] Neishtadt A. I., *Proc. Steklov Inst. Math.*, **250** (2005) 183.
[26] Shapere A. and Wilczek F. (Editors), *Geometric Phases in Physics* (World Scientific, Singapore) 1989.
[27] Holm D. D. and Lynch P., *SIAM J. Appl. Dyn. Syst.*, **1** (2002) 44.
[28] Sanrey M., Joyeux M. and Sadovskiĭ D. A., *J. Chem. Phys.*, **124** (2006) 074318.
[29] Pavlov-Verevkin V. E., Sadovskiĭ D. A. and Zhilinskiĭ B. I., *Europhys. Lett.*, **6** (1988) 573.